

Bifurcations in the Lozi map

V Botella-Soler[†], J M Castelo[‡], J A Oteo[§] and J Ros[†] ||

[†]Departament de Física Teòrica and IFIC, Universitat de València-CSIC,
46100-Burjassot, València, Spain

[‡] Departament de Física Aplicada, Universitat de València, 46100-Burjassot,
València, Spain

[§] Departament de Física Teòrica, Universitat de València, 46100-Burjassot, València,
Spain

E-mail: vicente.botella@uv.es, oteo@uv.es, rosj@uv.es

Abstract. We study the presence in the Lozi map of a type of abrupt order-to-order and order-to-chaos transitions which are mediated by an attractor made of a continuum of neutrally stable limit cycles, all with the same period.

PACS numbers: 05.45.Pq, 05.45 Ac, 02.30 Oz

AMS classification scheme numbers: 37G35, 37M05, 74H99, 37D45

Submitted to: *J. Phys. A: Math. Gen.*

9 January 2013

|| To whom correspondence should be addressed

1. Introduction

In 1978, Lozi introduced in a short note [1] a two-dimensional map the equations and attractors of which resemble those of the celebrated Hénon map [2]. Simply, a quadratic term in the latter is replaced with a piecewise linear contribution in the former. This allows one to rigorously prove the chaotic character of some attractors [3] and a detailed analysis of their basins of attraction [4]. The equations for the iterated Lozi map $L(x, y)$ read

$$\begin{aligned}x_{n+1} &= 1 + y_n - a|x_n| \equiv f(x_n, y_n) \\ y_{n+1} &= bx_n \equiv g(x_n, y_n),\end{aligned}\tag{1}$$

where a, b are real non-vanishing parameters. Inside the region where the orbits remain bounded, the Lozi map may present both regular and chaotic behavior.

The purpose of this article is to show that the Lozi map also exhibits a special type of bifurcation recently found in a class of one dimensional discontinuous piecewise linear maps [5]. A similar phenomenon in continuous maps was also described in [6]. The main feature of this bifurcation is the presence of a continuum of neutrally stable cycles. Thus, at the very bifurcation point, the attractor in phase space contains an infinite set of regular orbits. As a function of the parameters the transit may take place from regular to regular as well as to chaotic regimes.

In maps in one dimension this kind of transitions happens whenever a piece of an iterate of the map becomes co-linear with the identity function, the bisectrix, in the cobweb for a particular value of the parameter. We will extend this explanation to maps in two dimensions and discuss its connection with the theory of border collisions, which is commonly used to analyse these kinds of maps [7, 8, 9]. Very recently, this question has been considered from a more abstract point of view [10] and the name *degenerate bifurcation* has been used. As this term may sound polysemous we refer to this phenomenon as *bisecting bifurcation* in the rest of the paper, which seems more in accordance with the geometrical interpretation advanced.

An overview of the results on the Lozi map necessary for later reference is presented in section 2. Bisecting bifurcations are introduced and analysed in section 3. They are then given a geometrical explanation in section 4. In section 5 we further illustrate how the dynamics of the map changes with parameter a and establish a connection with the theory of border collisions. Section 6 contains some final comments on somewhat related topics.

2. Dynamics of the Lozi map: isolated attractors and stability

It is customary to start the study of a dynamical system with a catalogue of its fixed points, periodic attractors and so on, paying special attention to their stability and evolution with the system parameters. We start by collecting some of these features for the Lozi map which will be referred to in the following sections.

For stability considerations we need the Jacobian matrix of $L(x, y)$ which reads

$$J(x, y) = \begin{pmatrix} -a \operatorname{sign}(x) & 1 \\ b & 0 \end{pmatrix}. \quad (2)$$

Notice that $J(x, y)$ depends on the point of the orbit only through $\operatorname{sign}(x)$. Accordingly, we denote its values as $J_+ \equiv J(x > 0, y)$ and $J_- \equiv J(x < 0, y)$. Furthermore, since $\det J_{\pm} = -b$, we will only consider maps with $|b| \leq 1$, in order to have non-expanding systems. In particular, the maps with $b = \pm 1$ are area-preserving.

It is a simple exercise to see that for $|b| \leq 1$ the Lozi map has no fixed points if $a \leq b - 1$. It has P_1 as the unique fixed point if $b - 1 < a \leq 1 - b$, and gains an additional fixed point, P_2 , if $a > 1 - b$, with

$$P_1(a, b) \equiv \left(\frac{1}{1 + a - b}, \frac{b}{1 + a - b} \right) \quad P_2(a, b) \equiv \left(\frac{1}{1 - a - b}, \frac{b}{1 - a - b} \right). \quad (3)$$

Furthermore $J(P_1) = J_+$, $J(P_2) = J_-$. Only P_1 may be stable and this happens for systems with parameter values (b, a) inside the triangle with vertices $(1, 0)$, $(-1, 2)$, $(-1, -2)$ in parameter space.

As for isolated cycles of period $T = 2$, it is easy to see that they exist, if we keep $|b| < 1$, for $a > 1 - b$. Their elements are (z_1, bz_2) and (z_2, bz_1) , with

$$z_1 = \frac{1 - b + a}{(1 - b)^2 + a^2} \quad z_2 = \frac{1 - b - a}{(1 - b)^2 + a^2}. \quad (4)$$

They are stable for parameter values (b, a) inside the triangle with vertices $(0, 1)$, $(1, 0)$, $(1, 2)$ in parameter space.

The analysis so far is standard and may be pursued for more complicated attractors. We have recalled the previous facts just to better understand the bifurcations which will be studied in the next section.

3. Bisecting bifurcations and attracting sets

The fixed points and cycles mentioned above were isolated points in the phase space. However, for particular values of the parameters a and b we can also find continuum sets of periodic points which act as attractors for certain regions of phase space. We commence by explaining the approach we follow to locate algebraically which values of a and b give rise to such infinite sets of simultaneous cycles. We solve first the cases of periods two and four which we deem illustrate sufficiently the procedure. After that, we completely determine the cycles' elements. Period three and five are then analyzed in the same way and shown to produce a different pattern. The stability of the cycles is also resolved. Higher order periodic attractors may be studied along the same line, of course at the price of more involved algebra.

3.1. Continuum of period-2 attractors

Let $\{(x_1, y_1), (x_2, y_2)\}$ be a period-2 cycle of the Lozi map. Next, instead of (1) we use the equivalent second order difference equation

$$x_{n+1} = 1 - a|x_n| + bx_{n-1}, \quad (5)$$

with the obvious corresponding change in the initialization of the iteration. The periodicity condition for this system conveys

$$x_2 = 1 - a|x_1| + bx_2, \quad (6)$$

$$x_1 = 1 - a|x_2| + bx_1. \quad (7)$$

The corresponding 2-cycles of the Lozi map will be $\{(x_1, bx_2), (x_2, bx_1)\}$.

When the system of equations above is compatible but indeterminate then there exists an infinity of solutions and hence of period-2 cycles. From an algebraic point of view this means that the coefficient and the augmented matrices must both have rank one:

$$\begin{vmatrix} a \operatorname{sign}(x_1) & 1 - b \\ 1 - b & a \operatorname{sign}(x_2) \end{vmatrix} = 0, \quad \operatorname{rank} \begin{pmatrix} a \operatorname{sign}(x_1) & 1 - b & 1 \\ 1 - b & a \operatorname{sign}(x_2) & 1 \end{pmatrix} = 1, \quad (8)$$

which yield the constraints: $a > 0$ and either $b + a = 1$ or $b - a = 1$. Correspondingly there are two one-parameter families of 2-cycles in \mathbb{R}^2 , $\{S_1, S_2\}$ and $\{U_1, U_2\}$ with

$$S_1 = (x, b(1 - ax)/a), \quad S_2 = ((1 - ax)/a, bx), \quad (0 < x < 1/a, b = 1 - a) \quad (9)$$

$$U_1 = (x, -b(1 + ax)/a), \quad U_2 = (-(1 + ax)/a, bx), \quad (-1/a < x < 0, b = 1 + a). \quad (10)$$

For the S -family we have $J(S_1)J(S_2) = J_+^2$, whose eigenvalues are $(a^2 + 2b \pm |a|\sqrt{a^2 + 4b})/2$. In the critical case, $a + b = 1$, they reduce to the values 1 and $(1 - a)^2$, and hence these orbits are neutrally stable whenever $0 < a < 2$. Then the continuum they form is an attractor in phase space.

For the U -family we have $J(U_1)J(U_2) = J_-^2$, whose eigenvalues in the critical case, $b - a = 1$, are 1 and $(1 + a)^2 > 1$, with $a > 0$. Therefore these orbits are unstable.

3.2. Continuum of period-4 attractors

The search of sets of period-4 orbits yields the following results. First, the constraints on the parameters are $a = 1 + b$, and $0 < b < 1$, $1 < a < 2$, for the rank of the corresponding matrices to be equal to three, allowing in this way the existence of a one-parameter family of solutions. Second, if (x_i, y_i) denotes the cycle elements, with $i = 1, \dots, 4$, then

$$x_1 = \mu + 2b\beta, \quad x_2 = \mu - (b - 1)\beta, \quad x_3 = -\mu, \quad x_4 = -\mu + (b + 1)\beta, \quad (11)$$

$$y_1 = bx_4, \quad y_2 = bx_1, \quad y_3 = bx_2, \quad y_4 = bx_3, \quad (12)$$

where we have used the real parameter $0 < \mu < 1$ and the definition $\beta \equiv 1/(1 + b^2)$.

One can readily deduce from the expression of the cycle elements (11) that the x -components are alternatively positive and negative. Therefore the corresponding

Jacobian matrix reads simply $(J_+J_-)^2$, whose eigenvalues are 1 and $(1-a)^4$ in the critical case. Hence, these period-4 orbits are neutrally stable and their union acts also as an attractor.

3.3. Period-3 attractors

Following the same algebraic procedure as in the preceding subsections, we have determined that an infinite set of cycles of three elements exists only if $a = 1$ and $b = -1$. However, in this case the rank of the corresponding coefficient and augmented matrices is equal to one and, as a consequence, we get a continuum of solutions depending on two parameters.

A phase portrait which includes the period-3 orbits is shown in Figure 3. Orbits of period-3 fill completely the white triangle at the center of Figure 3, with right angle vertex at $(0,0)$. The acute angle vertices are located at $(1,0)$ and $(0,1)$. The elements of the cycle are given by $(\xi, -\eta)$, $(1 - \xi - \eta, -\xi)$ and $(\eta, -1 + \xi + \eta)$, in terms of the parameters $0 < \xi, \eta < 1$. The remaining white areas correspond to regular orbits of higher periods. Finally, the black and grey areas stand for chaotic trajectories.

The two eigenvalues of the Jacobian matrix of $L^{[3]}(x, y)$ evaluated on the orbit elements are equal to one, which stands for double neutral stability. Hence, the set of orbits of period-3 is two-dimensional in phase space, at variance with period-2 and -4, and is embedded into the sea of chaotic trajectories.

3.4. Period-5 attractors

The situation with period-5 attractors is similar to the one with period-3. We have found two two-parameter sets of orbits with neutral stability. They emerge when $b = -1$ and either $a = (1 + \sqrt{5})/2 \equiv \phi$ (the golden ratio) or $a = (1 - \sqrt{5})/2$. Table 1 collects the elements $\{x_i, y_i\}$, with $i = 1, \dots, 5$, of the orbit. We use the notation $\varphi \equiv (\sqrt{5} - 1)/2 = \phi - 1 = 1/\phi$. The two parameters u and v which define the family of period-5 orbits vary in the pentagon of vertices $\{(\varphi^2, 0), (\varphi, 0), (\varphi^2, \varphi^2), (0, \varphi), (0, \varphi^2)\}$ in parameter space, provided $a = \phi$. Else, if $a = -\varphi$, the two parameters vary in the pentagon of vertices $\{(0, 0), (1, 0), (\phi, 1), (1, \phi), (0, 1)\}$. As far as stability is concerned, a direct calculation shows that the Jacobian matrix of $L^{[5]}(x, y)$ for the parameter values just quoted is indeed the unit matrix which means double neutral stability.

3.5. Bifurcation diagrams

It is customary to summarize the behavior of a map with varying parameters by means of bifurcation diagrams. In principle there are two somewhat extreme ways to construct these diagrams. The ideal mode to proceed is clear: one determines by a theoretical analysis the periodic points and their stability and plot them as functions of a parameter. This is often impossible to carry out completely and then one has to resort to a more *experimental* way: iterate the map for a number of initial conditions, discard a transient

in the trajectories and plot then a component as a function of the parameter. The unavoidable limitations of the last approach are clear and one has to take special care to identify the results obtained. In particular, a densely filled bar in a diagram is usually taken as a signature of chaos.

In the Lozi map, when enough initial conditions are considered for the numerical simulation, the continua of 2– and 4–cycles discussed above may act as an attractor and show up also as a vertical line in the bifurcation diagram. This is clearly seen in Figure 1 for fixed $b = 0.1$. To construct this diagram especial care has been payed to sweep a large number of initial conditions. For every trajectory a large enough transient is discarded. Also, if a component increases beyond a given threshold the trajectory is considered as unbounded. Figure 1 exhibits a bifurcation from period–1 to period–2 at $a = 0.9$ and another one from period–2 to chaos at $a = 1.1$. This numerically obtained diagram illustrates clearly that these two bifurcations are mediated by the phenomena described in sections 3.1 and 3.2 respectively. A further feature of Figure 1 is that in the approximate intervals $1.1 < a < 1.237$ and $1.237 < a < 1.406$, the trajectories jumps between the chaotic bands in a cyclic manner, with periods 4 and 2 respectively.

Similarly, in Figure 2, here for fixed $a = 1.5$, two bifurcations occur at $b = \pm 0.5$, again mediated by the same mechanism. The system is chaotic for $b = 0.1$ and $a > 1.1$ in Figure 1, and $a = 1.5$, $-0.5 < b < 0.5$ in Figure 2. The presence of these vertical segments corresponding to the described attractors composed of infinite sets of periodic orbits is the most salient feature of the phenomenon we deal with here. We term it *bisecting bifurcations* for reasons which will appear clear in the next section. Eventually, cyclic jumping between the chaotic bands of the diagram takes place with period 2 and 4 to the left and right of the figure, respectively.

We gather the information discussed so far in Figure 4 where the behavior of the Lozi map in different regions of the parameter space is indicated. Trajectories for $|b| > 1$ are unbounded. Numerical simulations indicate this is also the case for the northern and southern parts of the diagram. The identification of the chaotic area has been achieved by computing numerically the Lyapunov exponents [11], thus the upper border of chaos

a	i	1	2	3	4	5
ϕ	x_i	$1 - \phi v - u$	$-\phi + \phi(u + v)$	$1 - \phi u - v$	u	v
	y_i	$-v$	$\phi v + u - 1$	$\phi - \phi(u + v)$	$\phi u + v - 1$	$-u$
$-\phi$	x_i	$1 + \phi v - u$	$\phi - \phi(u + v)$	$1 + \phi u - v$	u	v
	y_i	$-v$	$u - \phi v - 1$	$\phi(u + v) - \phi$	$v - \phi u - 1$	$-u$

Table 1. Elements of the period–5 orbits $\{x_i, y_i\}$, ($i = 1, \dots, 5$). The upper block entry is for $a = \phi$. The real parameters u, v take values inside and on the pentagon of vertices $\{(\phi^2, 0), (\phi, 0), (\phi^2, \phi^2), (0, \phi), (0, \phi^2)\}$ of parameter space. The lower block entry is for $a = -\phi$ and the parameters are inside and on the pentagon of vertices $\{(0, 0), (1, 0), (\phi, 1), (1, \phi), (0, 1)\}$ in parameter space. In both cases it is $b = -1$. All the orbits elements stay in the first quadrant of phase plane.

is approximate. The stable fixed points of L and $L^{[2]}$, are included in the graphics. The borders of their stability region will be analysed in detail later on. The diagram by no means exhausts the variety of behaviors the trajectories of the Lozi map may develop [12].

4. A geometrical explanation for the bisecting bifurcations in the Lozi map

In [5], a geometrical explanation for the bisecting bifurcations in piecewise one-dimensional maps is provided. Here we develop a generalization for the two-dimensional Lozi map, although the graphical illustration is more involved. Figure 5 represents the surface $f^{[4]}(x, y)$ and allows us to appreciate how the simple shape of $f(x, y)$ in (1) becomes convoluted after iteration.

Notice that for the Lozi map, the existence of a bisecting bifurcation in the variable x implies its presence in the variable y , and viceversa. This is due to the fact that y is just a one iteration delayed and re-scaled version of x . This observation will render easier the design and interpretation of some three dimensional diagrams.

From an algebraic point of view, we will find an infinity of period- n limit cycles if

$$f^{[n]}(x, y) = x, \quad g^{[n]}(x, y) = y, \quad (13)$$

for some range of (x, y) values, as illustrated for $n = 2$ to 5 in section 2. Clearly, this is the condition of fixed point extended to a continuous set of points in phase space. Furthermore, this is only a necessary condition for the observation of the infinity of limit cycles since its stability is not assured by it.

In one-dimensional maps it is a common practice to construct and study trajectories using the cobweb diagram. In a two-dimensional generalization we can visualize $f^{[n]}(x, y)$ and $g^{[n]}(x, y)$ as surfaces to which a point $p \equiv (x_m, y_m)$ of the phase plane is projected upward in order to find the new $x_{m+1} = f^{[n]}(x_m, y_m)$ and $y_{m+1} = g^{[n]}(x_m, y_m)$ on the vertical axis. This procedure is illustrated in Figure 6 for the particular case $n = 1$. The horizontal plane stands there for the phase plane. The vertical axis is common for both surfaces $f^{[n]}(x, y)$ and $g^{[n]}(x, y)$, which have been sketched only partially. Using the cobweb diagram technique, the values x_{m+1} and y_{m+1} are sent back to the phase plane. Thus, the value x_{m+1} is first projected toward the bisectrix line $f^{[n]}(x, 0) = x$ and then down to the x -axis. Similarly, y_{m+1} is first projected toward the bisectrix $g^{[n]}(0, y) = y$ and then down to the y -axis. This gives the point $q \equiv (x_{m+1}, y_{m+1})$ on the phase plane of Figure 6.

Let us now interpret condition (13) in geometrical terms. The presence in a two-dimensional map of a bifurcation mediated by an infinite set of neutrally stable cycles implies the existence of a segment, or set of segments, in the phase plane whose projections upward on the surfaces $f^{[n]}(x, y)$ and $g^{[n]}(x, y)$ are contained in the bisecting planes $f^{[n]}(x, y) = x$ and $g^{[n]}(x, y) = y$ respectively. This explanation justifies the name *bisecting bifurcation* we have given to the phenomenon we are discussing.

In the case of the Lozi map, f and g allow explicit solutions for condition (13) to be found, at least for low values of n . Next we focus on the particular case of the bifurcation

occurring at $a = 1 - b$ with $a > 0$. In this case the limit cycles at the bifurcation point are all period-2 cycles, i.e. fixed points of $L^{[2]}(x, y)$. In Figure 7 we have represented the surface $f^{[2]}(x, y)$ and the generalized cobweb procedure described above. For the sake of clarity, any analogous representation concerning $g^{[2]}(x, y)$ has been omitted. The plot has been generated for $b = 0.1$ and $a = 0.9$. Any initial condition (x_0, y_0) lands, after a certain transient, on the segment $y = b(1 - ax)/a$ with $0 < x < 1/a$ (red line in Figure 7). Every point of this segment is a fixed point of $L^{[2]}(x, y)$. When projected to the surface $f^{[2]}(x, y)$ they graze the bisector plane $f^{[2]}(x, y) = x$ and then come back to their position in the phase plane. Since this segment is invariant under the transformation $L^{[2]}(x, y)$, any point in the segment is an element of a period-2 cycle of $L(x, y)$.

In summary, from a three-dimensional geometrical perspective, we will find an infinite set of limit cycles of period n from the Lozi map when the projections on the phase plane of the two curves produced by the intersections of i) the surface $f^{[n]}(x, y)$ and the bisector plane $z = x$, and ii) the surface $g^{[n]}(x, y)$ and the bisector plane $z = y$, overlap in a certain range of the variables x, y . Whenever the intersection is not a linear segment but an area, the system has double neutrally stable orbits, which is the case of the period-3 and -5 orbits we have studied.

5. Bifurcations and phase space

In this section we discuss the appearance of the bisecting bifurcations in connection with the changes in the stability of other attractors. This will further clarify the meaning of the vertical segments in bifurcation diagrams like the ones in Figures 1 and 2. To be specific we fix $b = 0.5$ and plot in Figure 8 twenty regular attractors in phase space corresponding to parameter values $a = 0.1n$, $n = 1, 2, \dots, 20$.

The diagram allows us to appreciate how the fixed point attractor evolves with increasing a for $n = 1, \dots, 4$. At $a = 1 - b = 0.5$, i.e. $n = 5$, the first bisecting bifurcation takes place. Observe that this is precisely where the neutrally stable fixed point $P_1(a, b)$ in (3) changes to be unstable. We note in passing that this type of behavior sounds familiar from the analysis of elementary systems. For example, in the most conventional period-doubling cascade that would mean the birth of a period-2 attractor. Here something of this sort is also observed because 2-cycles exist to the right of $a = 0.5$. The difference is that the transition is mediated by a continuum of neutrally stable cycles of period-2 which fill up the segment in the figure.

When we continue to increase a the system is periodic with stable period-2 cycles. These have been represented in the figure for nine values of a , namely $n = 6, \dots, 14$. Then, at $a = 1 + b = 1.5$, the second bisecting bifurcation takes place. Again these parameters values punctuate the transition from stable to unstable for the 2-cycles mentioned in section 2. The two segments of the attractor are now built up by neutrally stable cycles of period-4, and they are apparent in Figure 8. Values $a > 1.5$ convey chaos (not shown) with unstable cycles in it ($n = 16, \dots, 20$).

The case considered illustrates, for fixed b and varying a , how the Lozi map follows

a route to chaos in three steps separated by two bifurcations characterized by the coexistence of a continuum of cycles with period 2 and 4 respectively. In Figure 4 this corresponds to a raising vertical trajectory in parameter space. As a matter of fact this figure contains information on the whole family of bifurcation diagrams like the ones in Figures 1 and 2 which stem from, respectively, vertical or horizontal displacements in parameter space. Accordingly, a variety of transitions are possible: fixed point to chaos, periodic cycle to chaos or fixed point to periodic cycle. We emphasize the role the bisecting bifurcations play in mediating these transitions.

Since piecewise continuous maps are usually analyzed in terms of border collisions [7, 8], it is appropriate to discuss the connection of the bisecting bifurcations with that scheme. In the particular case of the Lozi map, the described period-2 and period-4 attractors involving neutrally stable cycles may be seen as border collisions too. To see how this comes about we propose to look again at Figure 8 but going in the reverse direction. Starting with systems with $a = 2$ and progressively decreasing its value ($n = 20, \dots, 16$), one finds unstable period-4 orbits represented by circles. For $a = 1.5$ these cycles collide with the borders, namely the discontinuities of $L^{[4]}(x, y)$ (dashed lines), originating the two segments made of an infinite set of neutrally stable cycles of period-4. After the collision, further decrease of a gives then rise to stable period-2 attractors for $a < 1 + b = 1.5$. Following the way down, the 2-cycle collides, for $a = 1 - b = 0.5$, with the discontinuities of $L^{[2]}(x, y)$ and we see a sudden and ephemeral segment of period-2 neutrally stable cycles. Finally, for $a < 0.5$ we find the stable fixed points P_1 . Notice that in these collisions the location of the borders depends on a , except the one at $x = 0$ which is fixed.

As regards the chaotic regime, two examples of attractors appear in Figure 9, intended to be complementary of Figure 8. The upper panel is for $a = 1.55$ and shows an incipient zigzagged structure in phase space as the result of the destruction of the regular attractor $a = 1.5$ in Figure 8. In the bottom panel, with $a = 1.7$, the strange attractor is apparent. It corresponds to the figure in the original reference [1]. This V-shaped structure seems to be the prototype of chaotic attractor with $|b| < 1$. Points in the dotted pattern originate unbounded orbits.

So far in this section we have considered $|b| < 1$. As has already been mentioned, systems with $|b| = 1$ are area-preserving and their attractors offer a large variety of structures. Figure 3 is an instance of this. The system with $a = 1, b = -1$, contains doubly neutrally stable period-3 orbits embedded in chaos. In this regard, Figure 10 illustrates that this situation corresponds also to a border collision. It shows the evolution with a of six different fixed points of $L^{[3]}(x, y)$ (curves coded as dashed and dot-dashed lines). The remaining lines in the plot stand for borders. The collisions between fixed points and borders at $a = 1$ are clearly observed.

The phase space shown in Figure 3 exhibits a mixed structure of periodic and chaotic trajectories clusters. The complexity of the phase space is general for $|b| = 1$, even for non critical cases as $a = 1$. Figure 11 shows the phase space, at the same scale as Figure 3, of the neighbouring system $a = 0.9, b = -1$. Figure 12 shows the intricate phase space

structure in a larger scale. It is worth noticing that for conservative systems ($|b| = 1$) trajectories fill up densely any window in phase space. Thus, to obtain these kind of plots, one has to choose not only a large enough transient but also an adequate number of initial conditions and iterates to be plotted. Otherwise, the plot will hardly reveal inner structures.

6. Final comments

In this last section we mention some works related to the Lozi map which have some bearing with our results.

An interesting study of the dynamics of a Hénon–Lozi–type map is carried out in [13]. The authors introduce a C^1 smooth map which depends on a parameter ϵ . In the limit $\epsilon \rightarrow 0$ their map becomes the Lozi map, and they study which properties are preserved after the limiting procedure. In particular, they point out the interesting result that, whereas the smooth Lozi-like map presents a period-doubling route to chaos, the genuine Lozi map does not. This observation buttresses the interpretation advanced in the previous section. Instead of the common infinite sequence of successive period duplications, here we can observe a transition either from period 1 to 2 for $b > 1$, or none for $b < 1$, before entering the chaotic regime with the distinctive feature that at the bifurcation points there is an infinite set of neutrally stable cycles filling a segment, or a sector, in the phase plane.

The theory of border-collision bifurcations provides a classification and a description of the bifurcations caused by the collision of fixed points with boundaries in piecewise maps. This classification is based on the linearized version of the map around the collision point, usually called the *border-collision normal form map* [8]. However, when the normal form is written for the border collisions present in the Lozi map some of the non-degeneracy conditions assumed in the classification theorems do not apply [9]. In particular, the requirements related to the non-singularity of the coefficient matrices of the normal form map are not fulfilled. We refer to [9] for further mathematical details.

Important explicit results concerning systems with stable periodic orbits embedded in chaos have been reported in the literature. In particular, two works [14, 15] study in depth the area-preserving parameter-free maps

$$x_{n+1} = 1 - y_n \pm |x_n|, \quad y_{n+1} = x_n, \quad (14)$$

The former corresponds to the plus sign above and the latter to the minus sign, which is introduced because some calculations are considerably shorter. These two maps are, except for a reflection transformation ($y \rightarrow -y$), Lozi maps with $a = \pm 1, b = 1$. In [15] an infinite set of period-3 cycles, as the lowest period, are found embedded in a sea of chaos. They are essentially the ones we have reported in section 3.3. In [14] the analogue set is for orbits of period-6. In both cases further infinite sets of higher periods are studied too.

In this paper we have revisited the Lozi map with the purpose of showing that it presents what we have called bisecting bifurcations: those which are mediated by

an infinite set of neutrally stable periodic orbits. We have determined explicitly the location of some of them as well as their cycle elements. We have also provided an explanation for their existence in both algebraic and geometric terms. We deem that particular analyses, like the one we have carried out for the Lozi map, may help to enlarge our knowledge about the dynamics of piecewise continuous maps.

Acknowledgments

This work has been partially supported by contracts MCyT/FEDER, Spain FIS2007-60133 and MICINN (AYA2010-22111-C03-02). VBS thanks Generalitat Valenciana for financial support. The authors thank Joe Challenger for interesting comments on the manuscript.

References

- [1] Lozi R 1978 Un attracteur étrange (?) du type attracteur de Hénon *Journal de Physique* **39** C5–9
- [2] Hénon M 1976 A two-dimensional mapping with a strange attractor *Comm. Math. Phys.* **50** 69–77
- [3] Misiurewicz M 1980 Strange attractors for the Lozi mappings *Ann. N.Y. Acad. Sci.* **357** 348–358
- [4] Baptista D and Severino R 2009 The Basin of attraction of Lozi mappings *Int. J. Bifurcation Chaos* **19** 1043–1049
- [5] Botella-Soler V, Oteo J A and Ros J 2009 Dynamics of a map with a power-law tail *J Phys A: Math Theor* **42** 385101–23
- [6] Gardini L, Sushko I, Naimzada A. L. 2008 Growing through chaotic intervals *J Econ Theory* **143** 541–557
- [7] Nusse H E and Yorke J A 1992 Border-collision bifurcations including “period two to period three” for piecewise smooth systems *Physica D: Nonlinear Phenomena* **57** 39–57
- [8] Banerjee S, Grebogi C 1999 Border collision bifurcations in two-dimensional piecewise smooth maps *Phys. Rev. E* **59** 4052–61
- [9] Di Bernardo M, Budd C J, Champneys A R, Kowalczyk P 2008 Piecewise-smooth dynamical systems: theory and applications *Springer Verlag*
- [10] Sushko I, Gardini L, 2010 Degenerate bifurcations and border collisions in piecewise smooth 1D and 2D maps, *Int. J. Bifurcation Chaos*, 20, 7, 2045–2070
- [11] Alligood K T, Sauer T D and Yorke J A 1996 Chaos: an introduction to dynamical systems (Springer, NY)
- [12] Elhadj Z and Sprott J C 2010 A new simple 2-D piecewise linear map *J. Syst. Sci. Complex.* **23** 379–389
- [13] Aziz-Alaoui M A, Robert C and Grebogi C 2001 Dynamics of a Hénon-Lozi-type map *Chaos, Solitons and Fractals* **12** 2323–2341
- [14] Devaney R L 1984 A piecewise linear model for the zones of instability of an area-preserving map *Physica D* **10** 387–383
- [15] Aharonov D, Devaney R L and Elias U 1997 The dynamics of a piecewise linear map and its smooth approximation *Int. J. Bifurcation Chaos* **7** 351–372

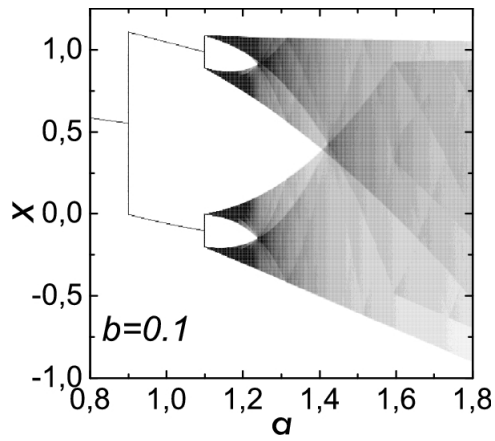


Figure 1. Bifurcation diagram for $b = 0.1$. Notice that the bisecting bifurcations take place at $a = 1 \pm b$.

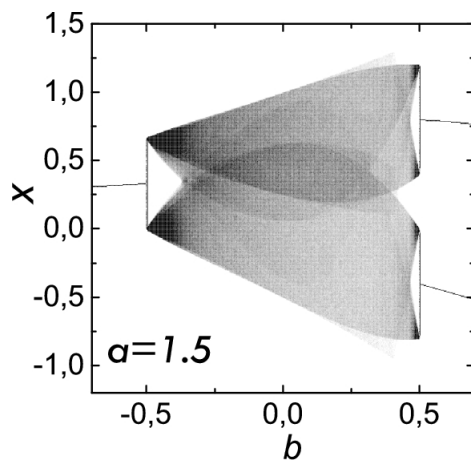


Figure 2. Bifurcation diagram for $a = 1.5$. Notice that the bisecting bifurcations take place at $b = \pm(a - 1)$.

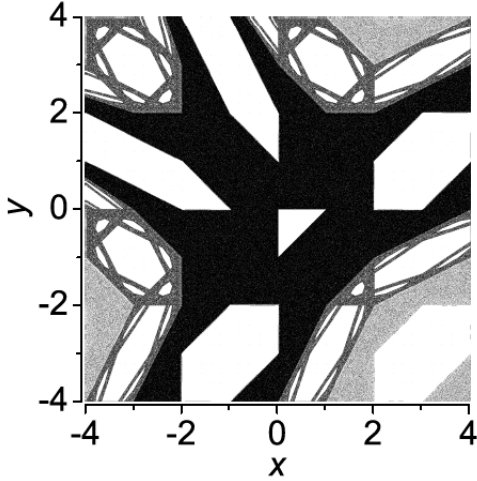


Figure 3. Attractor of the system $a = 1$, $b = -1$. Black and gray regions stand for chaotic trajectories. The white areas contain only periodic orbits with neutral stability. In particular, the innermost triangle with right angle vertex at $(0,0)$ contains only period-3 trajectories.

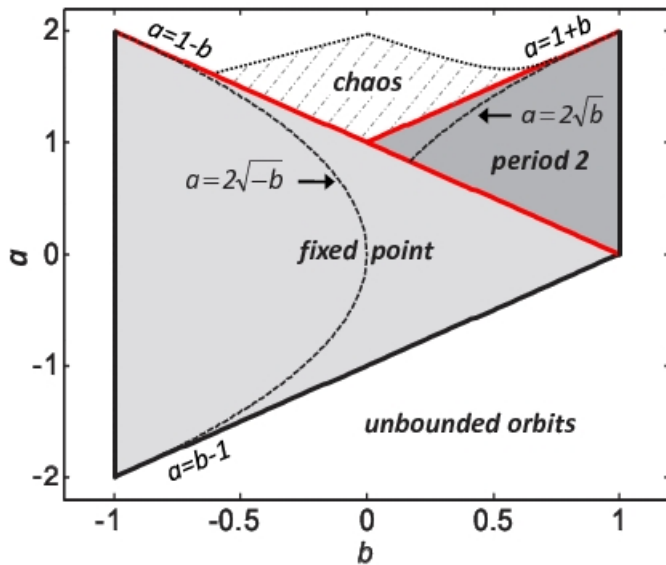


Figure 4. (Color online) Behaviour of the Lozi map in parameter space. White areas correspond to unbounded trajectories. The bisecting bifurcations take place at the red straight lines, $a = 1 \pm b$. This diagram does not exhaust all the possible attractors the Lozi map may exhibit.

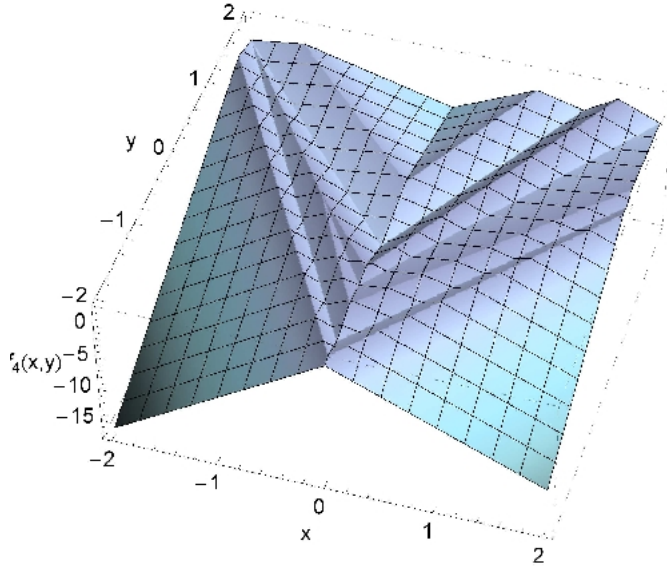


Figure 5. (Color online) Surface defined by the iterate $f^{[4]}(x, y)$ in the definition of the Lozi map, with $a = 1.5$ and $b = 0.5$.

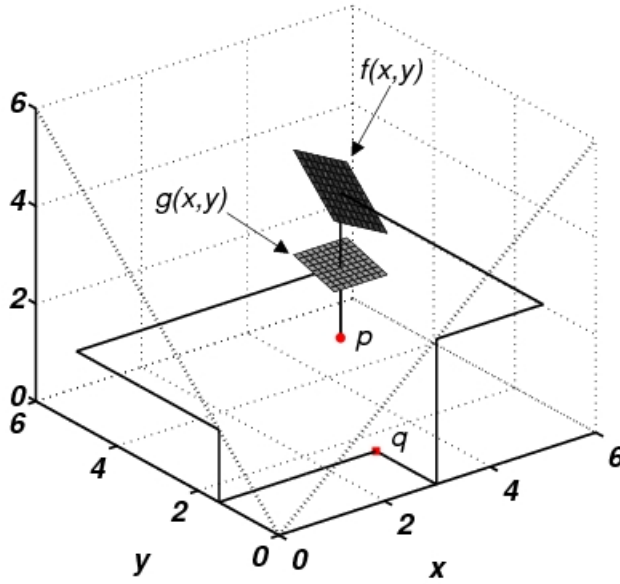


Figure 6. (Color online) Example of two-dimensional cobweb diagram for the Lozi map ($a = 0.6$, $b = 0.3$). The point $p \in \mathbb{R}^2$ is projected to the surfaces $f(x, y)$ and $g(x, y)$ and these projections are brought back down to \mathbb{R}^2 by means of reflections in the bisectrix $f(x, 0) = x$ and $g(0, y) = y$ in order to find the new point q . For the sake of clarity only one small region of each surface is shown.

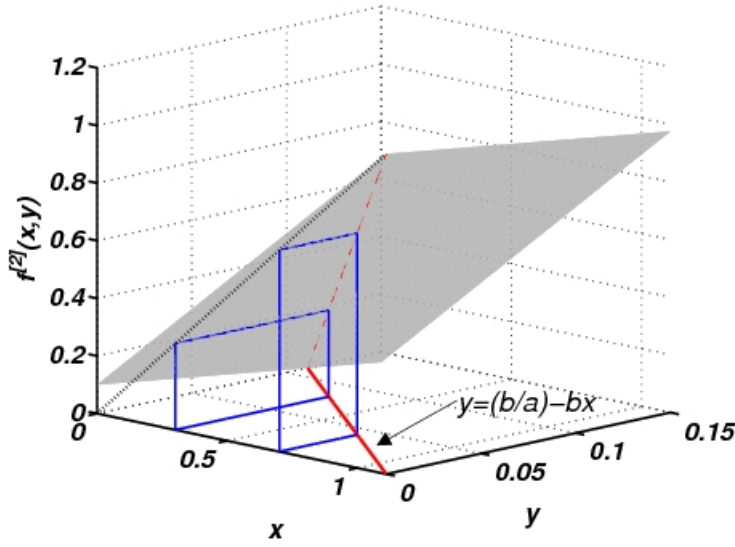


Figure 7. (Color online) Cobweb diagram for the 2nd iterate of the Lozi map with $b = 0.1$ and $a = 1 - b$. Only the $f^{[2]}(x, y)$ surface is shown. The cobweb trajectories (blue) of two different initial conditions ($x_0 = 0.3, 0.7$ and $y_0 = b(1 - x_0)/a$) have been represented.

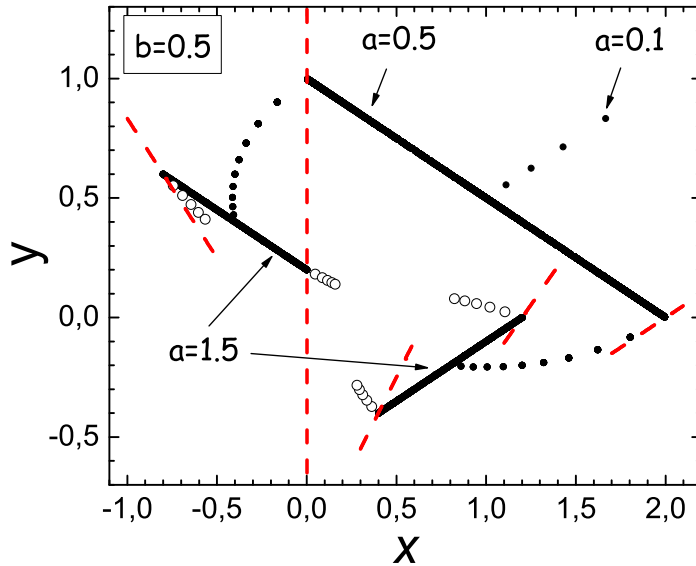


Figure 8. (Color online) Superposition of twenty attractors illustrating border collisions. $b = 0.5$ and $a = 0.1n$ with $n = 1, 2, \dots, 20$. Period-2 and period-4 attractors associated to neutrally stable orbits ($a = 0.5$ and 1.5) correspond to the segments (solid pattern). In between, stable period-2 limit cycles. The dashed lines stand for the borders at the bifurcation values (as a matter of fact, the border $x = 0$ is invariant). The circles stand for a period-4 unstable orbit plotted for the values $a = 0.1n$, $n = 16, \dots, 20$ which collides with the borders at the bifurcation.

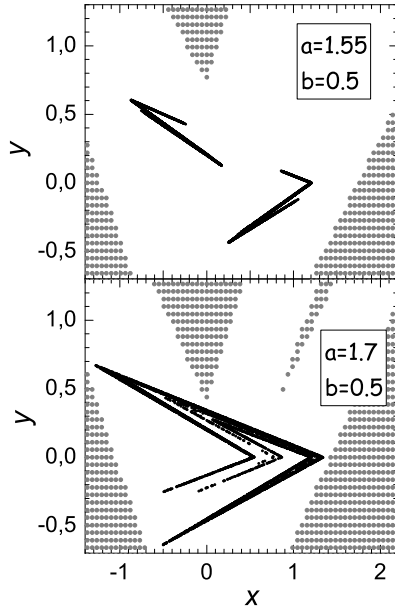


Figure 9. Two strange attractors of the Lozi map for the values a and b specified in the panels. Scales are the same as in Figure 8 what allows to appreciate how the regular attractor with $a = 1.5$ in Figure 8 becomes strange as a increases. Points in the dotted patterns give rise to unbounded orbits.

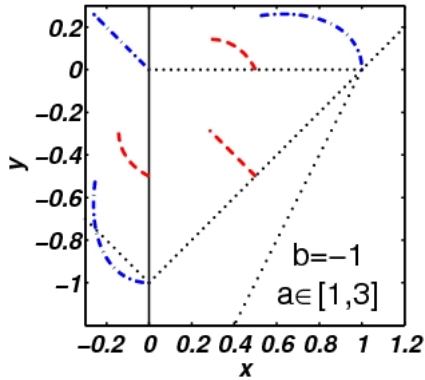


Figure 10. (Color online) Period-3 border collision in the Lozi map, illustrated as a sequence of snapshots in phase space. The solid line $x = 0$ stands for a border of the map, which is independent of a . The dotted lines represent further borders of the map at $a = 1, b = -1$. For other values of $a \neq 1$ these lines wander across the plot. The dashed and dot-dashed lines stand for the evolution of two different orbits of period-3 as the value of a varies in the interval $[1, 3]$. The border collision takes place at the bifurcation values $a = -b = 1$.

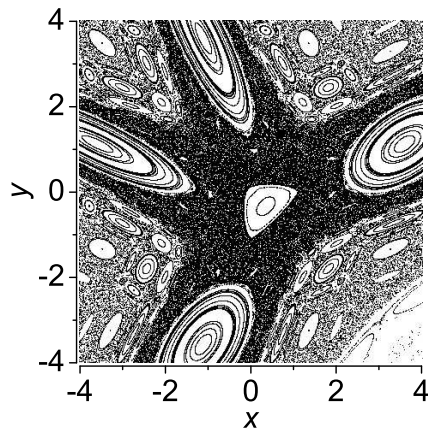


Figure 11. Phase space of the Lozi map for the values $a = 0.9$ and $b = -1$. Notice that the scales are the same as in Figure 3.

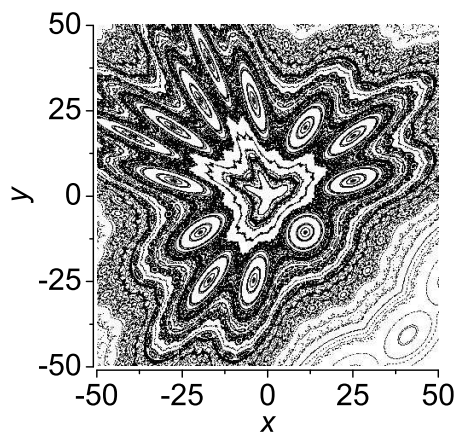


Figure 12. Phase space of the Lozi map for the values $a = 0.9$ and $b = -1$.